Modeling and Analysis of Biospecific Adsorption in a Finite Bath

A general model is presented and used to predict the dynamic behavior of the adsorption and wash stages of biospecific adsorption (affinity chromatography) in a finite bath. The model accounts for film and diffusional mass transfer resistances as well as for the rates of interaction between adsorbates and ligands. The model is applicable to single and multicomponent biospecific as well as nonspecific adsorption, and the adsorbates may be monovalent or multivalent. The predictions of the model are compared with the experimental data of the adsorption of β-galactosidase onto immobilized anti-β-galactosidase.

The results of biospecific adsorption of bivalent adsorbates indicate that a competition for ligands occurs between molecules forming one-site interaction and two-site interaction complexes. This competition can lead to the displacement of the adsorbate from the adsorbate-ligand complex whose formation is least favored.

B. H. Arve, A. I. Liapis
Department of Chemical Engineering
and Biochemical Processing Institute
University of Missouri
Rolla, MO 65401

Introduction

Recent advances in the areas of microbiology, molecular biology, immunology, and genetic and biochemical engineering have provided a wide range of different biochemical products that are or may become of great commercial value. Proteins and related substances are often the main constituents in many of these products, which may be used as pharmaceuticals and medical diagnostic reagents (Chase, 1984a). Many of these biochemical compounds are produced in biochemical reactors, and often the solution in the reactor is a complex biochemical mixture with the substances of interest present only in very small concentrations.

Many of the conventional separation processes (i.e., gel filtration, ion exchange, precipitation, ultrafiltration, electrophoresis) and their combinations (multistep purification procedures) may not be applicable to the purification of proteins from complex biochemical mixtures (Chase, 1984a). However, biospecific adsorption (affinity chromatography) seems to have the greatest potential for success in the very difficult task of purifying to homogeneity many biochemical substances from dilute mixtures containing a large number of proteins with small differences in solubilities, charges, and molecular sizes. This separation technique utilizes small differences in biological activities of molecules in order to achieve the purification of proteins. Often, very high degrees of purity as well as high product yields may be obtained in a single purification step.

The biospecific adsorption process is characterized by the immobilization of a selected biochemical or chemical compound (ligand) onto the internal surface of a porous, inert, solid support matrix. The ligand has a high, specific recognition of one particular compound or a class of components that are to be purified from a mixture involving many species. In the adsorption stage of the process the crude mixture containing the substance of interest (adsorbate) is contacted with the adsorbent and the desired protein binds reversibly to the immobilized ligands. The biological raw material that makes up the feed solution of the adsorption stage in most cases also contains other unwanted compounds, called contaminants, which are often present in quantities larger than those of the desired substance. During the adsorption stage some or all of the contaminants may diffuse into the porous particles, and depending on the type of solid matrix and ligand, it may be possible that one or more contaminants will be adsorbed biospecifically by the ligands or nonspecifically on the surface of the solid matrix (Chase, 1984a). In the wash stage the concentrations of the contaminants present within the porous adsorbent particles are reduced to a specified low level. Subsequently the adsorbate is recovered by promoting the dissociation of the adsorbate-ligand complex (elution stage), and finally the adsorbent is regenerated by contacting it with initial buffer solution (regeneration stage).

Very good reviews of biospecific adsorption are given by

Correspondence concerning this paper should be addressed to A. I. Liapis.

Porath and Kristiansen (1975), Chase (1984a), and Parikh and Cuatrecasas (1985). Janson and Hedman (1982), Hill and Hirtenstein (1983), and Janson (1984) have presented reviews of the principles, practical considerations, and industrial applications of biospecific adsorption. Chase (1984b) suggests a theoretical approach for the prediction of the performance of preparative biospecific adsorption separations for biological macromolecules in packed columns. Although the model of Chase (1984b) takes into account the reversible nature of the adsorbate-ligand interaction, it does not account for the mass transfer resistances within and around the particles. Therefore, this model lumps all the mass transfer resistances into the interaction rate constants; but it is well established that the transport of macromolecules in the pores of the adsorbent is a slow process. Arnold et al. (1985a, b) presented a model for biospecific adsorption in a batch system. They assumed that pore diffusion is the rate-determining step and that the rate of adsorption is very high, as well as that film diffusional resistance is negligible. However, there is evidence (Chase, 1984a, b; Arnold et al., 1985a, b) that the rate of biospecific adsorption may be a rate-limiting step, particularly when extremely small particles are used (Sportsman et al., 1983). A model for the wash stage in a batch system for the removal of a single contaminant was also presented by Arnold et al. (1985a). Using the approach of Carslaw and Jaeger (1959), a solution was presented when the rate-determining step is only the diffusion of the contaminant in the fluid of the pores. Film mass transfer resistance was not considered and the concentration of the contaminant at the start of the wash stage ($t_w = 0$) was assumed to be constant and uniform within the pores of the adsorbent particles. However, in practice the adsorption stage may be terminated before the concentration of the contaminant(s) reaches a constant and uniform concentration level within the pores of the adsorbent particles; thus the initial concentration profile of the contaminant(s) for the wash stage could be nonuniform.

Conclusions and significance of present work

General equations are presented to describe single and multicomponent biospecific as well as nonspecific adsorption from a finite bath onto porous adsorbent particles whose internal surface is covered by immobilized ligands. External film resistance and diffusional resistance within the particle are both included, and rate expressions for the interaction of the adsorbate and ligand are presented. The model presented in this work is applicable to systems having adsorbates that have only one site of interaction with the ligand (monovalent), as well as to biospecific adsorption processes whose adsorbates have multiple sites of interaction (multivalent) and therefore each adsorbate molecule may attach itself to more than one ligand. The method of orthogonal collocation was used to solve the equations of the model.

The predictions of the model presented in this work are compared with the experimental batch data of the adsorption of β-galactosidase, as well as with the predictions of other models presented in the literature. It is found that the model of this work could predict the experimental data more accurately than the other models for the whole duration of the biospecific adsorption process. The results indicate that the formation of the β-galactosidase/anti-β-galactosidase complex can be described by a second-order reversible interaction rate expression, and the film and pore diffusion mass transfer resistances cannot be ignored. Since the interaction rate mechanism and the intraparticle mass transfer mechanism in the adsorbent particles should be the same in both finite bath and column adsorption systems, an information flow diagram is presented which indicates that one may predict the behavior of biospecific adsorption in a column only from experimental batch data and appropriate batch and column models. Certain characteristic parameters that influence significantly the behavior of biospecific adsorption have been identified; they include the Sherwood, Porath, and adsorbate-ligand dissociation parameters.

The results of biospecific adsorption of bivalent adsorbates indicate that a competition for ligands occurs within the adsorbent particles between molecules forming one-site interaction and two-site interaction complexes. This competition for ligands leads, as time progresses, to the displacement of the adsorbate from the adsorbate-ligand complex whose formation is least favored.

The quantitative study of the wash stage indicates that in certain systems involving monovalent and bivalent adsorbates, the amount of product lost during the wash stage may be significant if the operation is terminated at early times. It is also shown that in order to satisfy a specified high level of product purity more than one wash may be required, and the number of washes, the overall wash time, and the amount of product lost during the wash stage depend on the criterion used to terminate each wash in the wash stage. The results suggest that the procedure selected to be used in the wash stage will involve a compromise between the number of washes required to achieve a given product purity and the amount of product that would be accepted to be lost during the required overall wash time.

System Description

In this work, biospecific adsorption in a finite bath is considered. This mode of operation may be advantageous when the raw material contains solid contaminants and cell debris that may be difficult to remove and which may interrupt a column process by clogging the bed (Porath and Kristiansen, 1975; Chase, 1984a; Frej et al., 1986). Experimental data obtained from batch systems may be used together with model predictions in order to estimate values of the parameters characterizing certain mass transfer mechanisms as well as the interaction rates of the adsorbate-ligand complex (Liapis and Rippin, 1978; Chase, 1984b). Some of these estimated parameter values may then be used in column models in order to predict the dynamic behavior of biospecific adsorption in packed beds. This approach may eliminate many tedious, expensive, and time-consuming column experiments.

Biospecific adsorption may be divided into two main groups as follows:

1. *Single-component Adsorption.* In this case a ligand is used which has a high biospecific recognition of only one species (Janson, 1984). Therefore, such a ligand will remove only one component of a complex mixture. Single-component adsorption may also occur when group-specific or "general" ligands (Janson, 1984) are used and the composition of the feed solution is such that only one species is adsorbed by the ligands.

2. *Multicomponent Adsorption.* When group-specific ligands are used, several closely related compounds may interact

with the ligand. Less specific adsorbents are obtained when more general ligands are employed.

The contaminants, on the other hand, may be divided into four groups according to their interaction with the adsorbent:

1. Contaminants that do not diffuse into the adsorbent, such as cell debris
2. Species that simply diffuse in the fluid of the pores but which are not adsorbed by either nonspecific or biospecific adsorption
3. Contaminants that diffuse into the particles and are adsorbed nonspecifically to the solid support matrix
4. Species that diffuse into the particles and compete with the solute(s) of interest for the ligands

Contaminants belonging to the first group may be separated from the adsorbent particles by centrifugation and filtration or by extraction in an aqueous two-phase system (Frej et al., 1986). Removal of contaminants that belong to the second group is accomplished by resuspending the adsorbent particles in a weak buffer solution which allows the contaminants to diffuse from the porous particles into the surrounding bulk phase solution. If the total amount of contaminants present within the pores of the adsorbent particles is large and a high product purity is required, then more than one wash may be necessary in order to reduce the concentrations of the contaminants to a low level. For the removal of contaminants that belong to the third or fourth group, washing with a weak buffer solution may not be sufficient and more effective methods, which may be equivalent to mild elution, may have to be employed (Chase, 1984a).

In this paper the adsorption stage of biospecific adsorption is studied. The work also includes a quantitative study of the wash stage when weak buffer solutions are used as washing media.

Mathematical Formulation of Biospecific Adsorption in a Finite Bath

Adsorption stage

In the adsorption stage the following mass transfer and interaction steps may be considered to occur in series:

1. The transport of adsorbate(s) from the bulk fluid to the external surface of the particle
2. The transport of adsorbate(s) within the porous particle
3. The interaction between the adsorbate(s) and the immobilized ligand

The interaction step may be composed of several substeps, depending on the complexity of the adsorbate-ligand interaction, and could include the binding of multivalent adsorbates to monovalent ligands (Eilat and Chaiken, 1979).

Adsorption is considered in a finite bath containing n components, and m ($m < n$) solutes may compete for the available ligands, which are considered to be uniformly immobilized on the internal surface of spherical, porous particles that have uniform size and homogeneous structure. It is also taken that $m + 1 \le i \le \ell$ ($\ell < n$) solutes may bind to the support matrix by nonspecific adsorption, and that $\ell + 1 \le i \le n$ solutes simply diffuse into the particles without interacting with the adsorbent. The porous particles are suspended in the liquid by agitation so that the liquid has free access, and the bulk phase concentration is taken to be uniform throughout the bath except in a thin film of liquid surrounding each particle. The adsorption process is considered to be isothermal, and the differential mass balance equation for each component $i = 1, 2, \ldots, m, \ldots, \ell, \ldots, n$ in the bulk fluid phase of the bath is given by the following dimensionless expression:

$$\frac{dC'_{di}}{d\tau} = 6\pi\left(\frac{1-\epsilon}{\epsilon}\right)\epsilon_p Sh_{pi} D_{pRi} \cdot \left(C'_{pi}\Big|_{\rho=1} - C'_{di}\right), \qquad i = 1, \ldots, n \quad (1)$$

where

$$Sh_{pi} = \frac{2R_o K_{fi}}{\epsilon_p D_{pi}} \qquad i = 1, \ldots, n \quad (2a)$$

$$D_{pRi} = D_{pi}/D_{p1} \qquad i = 1, \ldots, n \quad (2b)$$

The transport of solutes within the adsorbent is considered to be governed by diffusion of the species in the liquid phase of the pores. The off-diagonal elements of the effective pore diffusivity matrix are taken to be zero, since for dilute solutions (as are the solutions used in biospecific adsorption) Liapis and Litchfield (1981) have shown that the off-diagonal terms are much smaller than the diagonal elements. By setting the off-diagonal terms equal to zero the error introduced in the prediction of the behavior of an adsorption system is not significant. Taking the effective pore diffusivities to be constant, the transport equations for the solutes in the pores of the adsorbent particles are given by the following dimensionless expressions:

$$\frac{\epsilon_p D_{p1}}{A_o}\frac{\partial C'_{pi}}{\partial \tau} + \frac{C_T}{C_{doi}}\frac{D_{p1}}{A_o}\frac{\partial C'_{si}}{\partial \tau} = \frac{\epsilon_p D_{pi}}{R_o^2}\left(6\frac{\partial C'_{pi}}{\partial \rho} + 4\rho\frac{\partial^2 C'_{pi}}{\partial \rho^2}\right), \quad i = 1, 2, \ldots, m \quad (3a)$$

$$\frac{\epsilon_p D_{p1}}{A_o}\frac{\partial C'_{pi}}{\partial \tau} + \delta\frac{C^*_{soi}}{C_{doi}}\frac{D_{p1}}{A_o}\frac{\partial C'_{si}}{\partial \tau} = \frac{\epsilon_p D_{pi}}{R_o^2}\left(6\frac{\partial C'_{pi}}{\partial \rho} + 4\rho\frac{\partial^2 C'_{pi}}{\partial \rho^2}\right), \quad i = m+1, m+2, \ldots, \ell, \ell+1, \ell+2, \ldots, n \quad (3b)$$

In Eq. 3b when $\delta = 1$, species $i = m + 1, m + 2, \ldots, \ell$ are nonspecifically adsorbed; and when $\delta = 0$, components $i = \ell + 1, \ell + 2, \ldots, n$ diffuse in the particles without interacting with the adsorbent. Because of the commonly employed low density of immobilized ligand on the support matrix (Hill and Hirtenstein, 1983; Chase, 1984a), Eq. 3a does not account for surface diffusion since this mode of diffusion will not contribute significantly to the transport of solutes within the particles. In Eq. 3b surface diffusion for the nonspecifically adsorbed species is not considered since there is no evidence in the literature that it influences the dynamic behavior of biospecific adsorption systems. The initial and boundary conditions for Eq. 1, 3a, and 3b are given by

$$C'_{di} = 1 \text{ at } \tau = 0, \quad i = 1, \ldots, n \quad (4)$$

$$C'_{pi} = 0 \text{ at } \tau = 0, \quad i = 1, \ldots, n \quad (5)$$

$$C'_{si} = 0 \text{ at } \tau = 0, \quad i = 1, \ldots, m \quad (6)$$

$$C'_{si} = 0 \text{ at } \tau = 0, \quad i = m + 1, \ldots, \ell \quad (7)$$

$$\frac{\partial C'_{pi}}{\partial \rho} = \frac{Sh_{pi}}{4}\left(C'_{di} - C'_{pi}\Big|_{\rho=1}\right) \quad \text{at } \rho = 1, i = 1, \ldots, n \tag{8}$$

$$\frac{\partial C'_{pi}}{\partial \rho} = 0 \quad \text{at } \rho = 0, i = 1, \ldots, n \tag{9}$$

Since many of the compounds that are to be purified by biospecific adsorption have high molecular weights (1,000–500,000 or more) and are large in size, the interaction step may be so slow that it competes with the mass transfer steps in being the rate-limiting step (Chase, 1984a). The interaction between unbound adsorbate in the pore fluid A_i and vacant immobilized ligand L is considered to be of the form

$$A_i + L \underset{k_{2,i}}{\overset{k_{1,i}}{\rightleftharpoons}} A_i L, \quad i = 1, \ldots, m \tag{10}$$

where $A_i L$ represents the adsorbate-ligand complex. Then assuming elementary interactions, the rate of the adsorption step may be described by the following second-order reversible interaction

$$\frac{\partial C'_{si}}{\partial \tau} = \epsilon_p Po_i D_{pRi}\left[C_{doi} C'_{pi}\left(1 - \sum_{j=1}^{m} C'_{sj}\right) - K_{Di} C'_{si}\right], \quad i = 1, \ldots, m \tag{11}$$

where

$$Po_i = k_{1,i} A_o / \epsilon_p D_{pi} \quad \text{and} \quad K_{Di} = k_{2,i}/k_{1,i} \tag{12}$$

We call the parameter Po the Porath parameter in honor of Professor J. Porath who, together with his coworkers at Uppsala University, Sweden, has made some of the most significant contributions in the field of affinity chromatography (biospecific adsorption). It is worth noting that the Porath parameter may be seen to provide a measure of the speed of the adsorbate-ligand association step relative to the diffusion of the adsorbate in the pore. Also, the Porath parameter has units of cm^3/mg in the case of a second-order interaction and would be dimensionless for a first-order interaction. Therefore, it is worth noting that the dimensions of the Porath parameter depend on the order of the interaction rate.

In certain systems the rate of interaction may be much higher than the rates of mass transfer, and in such systems it may be assumed that equilibrium exists between the adsorbate and the adsorbate-ligand complex at each point in the pores. The accumulation on the pore surface is then given by the expression

$$\frac{\partial C'_{si}}{\partial \tau} = \sum_{j=1}^{m}\left(\frac{\partial f_i}{\partial C'_{pj}}\frac{\partial C'_{pj}}{\partial \tau}\right), \quad i = 1, \ldots, m \tag{13}$$

where

$$C'_{si} = f_i(C'_{p1}, \ldots, C'_{pm}), \quad i = 1, \ldots, m \tag{14}$$

The functions f_i represent the adsorption isotherms for the species that may compete for the available ligands. The equilibrium adsorption isotherm between the adsorbates in the pore fluid phase and the adsorbate-ligand complexes is often described by the Langmuir isotherm (Chase, 1984b; Arnold et al., 1985a, b) whose form in dimensional variables is

$$C_{si} = \frac{K_{Ai} C_T C_{pi}}{1 + \sum_{j=1}^{m} K_{Aj} C_{pj}}, \quad i = 1, \ldots, m \tag{15}$$

where $K_{Ai} = 1/K_{Di}$, and C_T represents the total concentration of available ligand. Equation 15 may be derived from the dimensional form of Eq. 11, and this implies that when the adsorbate-ligand interaction can be expressed by a second-order reversible interaction then, as the interaction rate becomes very large, Eq. 15 becomes an upper limit representing infinitely fast adsorption.

Another limiting case is obtained from Eq. 11 when $k_{1,i}/k_{2,i} \gg 1$, which implies that the adsorbate-ligand interaction is irreversible, that is

$$\frac{\partial C'_{si}}{\partial \tau} = \epsilon_p Po_i D_{pRi} C_{doi} C'_{pi}\left(1 - \sum_{j=1}^{m} C'_{sj}\right), \quad i = 1, \ldots, m \tag{16}$$

Equation 16 represents a limiting case of an adsorbate-ligand interaction with a very small dissociation constant K_{Di}. It should be noted that although the adsorbate-ligand interaction may be taken to be irreversible during the adsorption and wash stages, this does not prevent the disruption of the adsorption complex during the elution stage by means of an appropriate elution method (Chase, 1984a). The rate expressions that may describe the dynamics of the adsorption step of the nonspecifically adsorbed species $i = m + 1, m + 2, \ldots, \ell$, could have forms similar to those presented above for the biospecifically adsorbed species.

The cases treated above consider only monovalent adsorbates. However, many of the adsorbates of interest may have more than one active site and therefore these adsorbates have the possibility of attaching themselves to more than one ligand (Eveleigh and Levy, 1977; Eilat and Chaiken, 1979; Chase, 1984a, b). For single-component adsorption with an adsorbate A having a maximum number of z available sites, the following interactions with vacant ligands L are considered

$$\begin{aligned}
A + L &\underset{k_{2,1}}{\overset{k_{1,1}}{\rightleftharpoons}} AL_1 \\
AL_1 + L_{adj} &\underset{k_{4,1}}{\overset{k_{3,1}}{\rightleftharpoons}} AL_2 \\
&\;\;\vdots \\
AL_{z-1} + L_{adj} &\underset{k_{2z,1}}{\overset{k_{2z-1,1}}{\rightleftharpoons}} AL_z
\end{aligned} \tag{17}$$

where L_{adj} represents an adjacent vacant ligand and $AL_1, \ldots, AL_z$ represent the adsorbate-ligand complexes. Assuming that each interaction is elementary, and adopting an argument similar to that of Hougen and Watson (1947), the dimensionless rate equations for the multivalent interaction model may be written

as

$$\frac{\partial C'_{s1,1}}{\partial \tau} = \epsilon_p Po_{1,1}\left\{C_{do1}C'_{p1}\left[1 - \sum_{j=1}^{z} j(C'_{s1,j})\right] - K_{D1,1}C'_{s1,1}\right\} - \frac{\epsilon_p Po_{1,2}}{C_T}\left\{C'_{s1,1}C_T\left[1 - \sum_{j=1}^{z} j(C'_{s1,j})\right] - K_{D1,2}C'_{s1,2}\right\}$$

$$\frac{\partial C'_{s1,z}}{\partial \tau} = \frac{\epsilon_p Po_{1,z}}{C_T}\left\{C'_{s1,z-1}C_T\left[1 - \sum_{j=1}^{z} j(C'_{s1,j})\right] - K_{D1,z}C'_{s1,z}\right\} \quad (18)$$

where

$$Po_{1,1} = k_{1,1}A_o/\epsilon_p D_{p1}$$

$$Po_{1,2} = k'_{3,1}A_o/\epsilon_p D_{p1} \quad \text{and} \quad k'_{3,1} = k_{3,1}S$$

$$Po_{1,z} = k'_{2z-1,1}A_o/\epsilon_p D_{p1} \quad \text{and} \quad k'_{2z-1,1} = k_{2z-1,1}S \quad (19)$$

The dimensionless concentration of vacant adjacent ligand, $C'_{L_{adj}}$, is given by the following expression,

$$C'_{L_{adj}} = \frac{S}{C_T}C'_L \quad (19a)$$

Therefore, $Po_{1,1}$ has units of cm^3/mg while $Po_{1,j}(j = 2, \ldots, z)$ is dimensionless. The initial condition of Eq. 18 is

$$C'_{s1,j} = 0 \quad \text{at } \tau = 0, j = 1, 2, \ldots, z \quad (20)$$

Wash stage

The mass transfer and interaction mechanisms active during the adsorption stage are also considered to be active during the wash stage. Therefore, the wash stage may be described by the same material balance equations and boundary conditions used to model the adsorption stage. However, the initial conditions of the expressions that describe the dynamic behavior of the solutes in the finite bath, Eq. 1, during the wash stage become

$$C'_{di} = 0 \quad \text{at } \tau_w = 0, \quad i = 1, 2, \ldots, m, \ldots, \ell, \ldots n \quad (21)$$

The initial conditions of the pore diffusion model, Eqs. 3a and 3b, are as follows for the wash stage:

$$C'_{pi} = p_i(\rho) \quad \text{at } \tau_w = 0, i = 1, 2, \ldots, m, \ldots, \ell, \ldots, n \quad (22)$$

$$C'_{si} = q_i(\rho) \quad \text{at } \tau_w = 0, i = 1, 2, \ldots, m, \ldots, \ell \quad (23)$$

$$C'_{s1,j} = u_j(\rho) \quad \text{at } \tau_w = 0, j = 1, 2, \ldots, z \quad (24)$$

The functions $p_i(\rho)$, $q_i(\rho)$, and $u_j(\rho)$ provide the concentration profiles at the end of the adsorption stage for solutes in the pore fluid, adsorbed species, and a multivalent solute interacting with j sites, respectively.

The present work will only consider contaminants that belong to group 2, as identified in the System Description section, above. This implies that the adsorbent particles do not bind material by nonspecific adsorption and that none of the contaminants competes with the solute of interest for the ligands. The two mass transfer resistances considered in the transport of the contaminants are film and pore diffusion.

The details of the derivations for the models of the adsorption and wash stages are given in Arve (1986).

Numerical solution procedure

The method of orthogonal collocation (Villadsen and Michelsen, 1978) was applied with respect to the space variable of the partial differential equations of the model presented in the above sections, and the resulting nonlinear ordinary differential equations were integrated together with the ordinary differential equations of the material balances in the finite bath by using a third-order semiimplicit Runge-Kutta method (Michelsen, 1976). Jacobi orthogonal polynomials were used and it was found that an approximation order $N = 8$ proved to be sufficient in obtaining solute concentrations differing only in the fourth decimal place when compared with those obtained by higher approximations (Arve, 1986).

Results and Discussion

Adsorption stage

In order to use the model equations presented in this work and predict the dynamic behavior of biospecific adsorption in a finite bath, one should have estimates of the values of the parameters in the model. The values of ϵ_p, R_o, and ϵ may be easily obtained, but ϵ_p may have to be determined after the ligands have been immobilized on the support matrix, since the porosity may change when voluminous ligands are used. Values for the equilibrium dissociation constants K_{Di}, and the total concentration of available ligands C_T, may be obtained through equilibrium and adsorption/desorption experiments (Chase, 1984a, b). Estimates of the film mass transfer coefficients K_{fi} may be obtained from correlations given in the literature (Calderbank and Moo-Young, 1961; Calderbank and Jones, 1961; Blakebrough, 1967; Geankoplis, 1983). It should be noted that the correlations for the K_{fi} may not be valid for biochemical compounds of high molecular weight, and therefore they should be used with caution. The effective pore diffusivities D_{pi}, and the forward interaction rate constants $k_{1,i}$ [or $k_{2j-1,1}(j = 1, 2, \ldots, z)$ when an adsorbate with multiple sites interacts with ligands], may be obtained by using parameter estimation methods (Seinfeld and Lapidus, 1974; Klaus, 1981) that would be employed to match in an optimal way the predictions of the finite bath model with sets of experimental data, as shown in the information flow chart of Figure 1. Subsequently, the batch model may be used to predict the behavior of biospecific adsorption in the finite bath under various conditions of design and operation, Figure 1. It should be noted that if the effective pore diffusivities could be measured by independent experiments, (Geankoplis, 1983), then only the forward interaction rate constants should have to be estimated. Nygren and Stenberg (1985) have performed experimental studies on the kinetics of antibody-binding to surface-immobilized antigen by using ellipsometry and enzyme-

linked immunosorbent assay (ELISA) methods. It is suggested that a proper analysis of their experimental data may provide estimates of the forward interaction rate constants. Therefore, it appears that the forward interaction rate constants may be estimated by the procedure discussed in Figure 1 or from independent experiments such as those performed by Nygren and Stenberg (1985). It is also worth noting that the interaction constants of adsorbates interacting with immobilized ligands may differ in magnitude when compared with the interaction constants of the same adsorbate-ligand system where the ligand is in free solution (Porath and Kristiansen, 1975; Nygren and Stenberg, 1985).

The pore diffusion transport and adsorbate-ligand interaction mechanisms of biospecific adsorption in a finite bath should be the same as those of biospecific adsorption in a column (Chase, 1984a, b; Balzli et al., 1978; Tsou and Graham, 1985). Therefore, one could use in an appropriate column model the estimated values of D_{pi} and $k_{1,i}$ or D_{pi} and $k_{2j-1,1}$ obtained from batch experiments together with the values of axial diffusivities and column film mass transfer coefficients estimated from literature correlations (Liapis and Rippin, 1978), and predict the dynamic behavior of biospecific adsorption in a column as shown in Figure 1. The information flow diagram in Figure 1 presents a convenient procedure that may be used to predict the behavior of biospecific adsorption in a finite bath or in a column. This procedure uses information from correlations in the literature and batch experimental data. The batch experiments are easier, less expensive, and faster to perform than column experiments (Balzli et al., 1978; Chase, 1984a). The approach presented in Figure 1 does not suffer from the limitations of pulse analysis and HETP (height equivalent to a theoretical plate) theory (Arnold et al., 1985b), and may be considered to be generally applicable in the analysis and design of biospecific adsorption systems.

The procedure presented above was used in a simple model discrimination and parameter estimation study using the experimental batch data of Chase (1984b). The experiments examined the adsorption of β-galactosidase (molecular weight 464,000) onto anti-β-galactosidase immobilized on a porous silica support matrix. The values of certain known and estimated parameters for this system are given in Table 1.

In Figure 2 the batch experimental data for the adsorption of β-galactosidase onto anti-β-galactosidase (Chase, 1984b) are shown together with the predictions of various models; Chase (1984b) provides no information regarding the accuracy of his experimental data. Curve *1* represents the predictions obtained from the model of Chase (1984b), which accounts for the forward and backward interaction steps of the adsorbate-ligand complex, and ignores the mass transfer resistance in the pores and in the fluid film surrounding the adsorbent particles. Curve *2* shows the predictions of the pore-diffusion model presented in this work; the interaction between the adsorbate and ligand is described by a second-order reversible interaction, Eq. 11. The parameters D_{p1} and $k_{1,1}$ for the model of curve *2* were estimated simultaneously using a nonlinear least-squares method (Seinfeld and Lapidus, 1974, p. 346) and the experimental data shown in Figure 2, while the film mass transfer coefficient K_{f1} (Table 1) was estimated from a literature correlation (Geankoplis, 1983, p. 440). Curves *3* and *4* present the predictions of the pore-diffusion model of this work when the adsorbate and the complex are in equilibrium at each point in the pore, and the equilibrium isotherm is given by the Langmuir expression, Table 2. The differences between curves *3* and *4* occur because the data in curve *3* were obtained by estimating simultaneously (using the same method as in curve *2*) both K_{f1} and D_{p1}, whereas the data of curve *4* were predicted by estimating only D_{p1} and using the literature correlation shown in Table 2 to obtain a value for K_{f1}. The estimated values of the parameters used to obtain curves *2–4* are shown in Table 2.

In Figure 2 it can be observed that the best agreement between theory and experiment is obtained, throughout the adsorption process (in time), by the pore-diffusion model of this

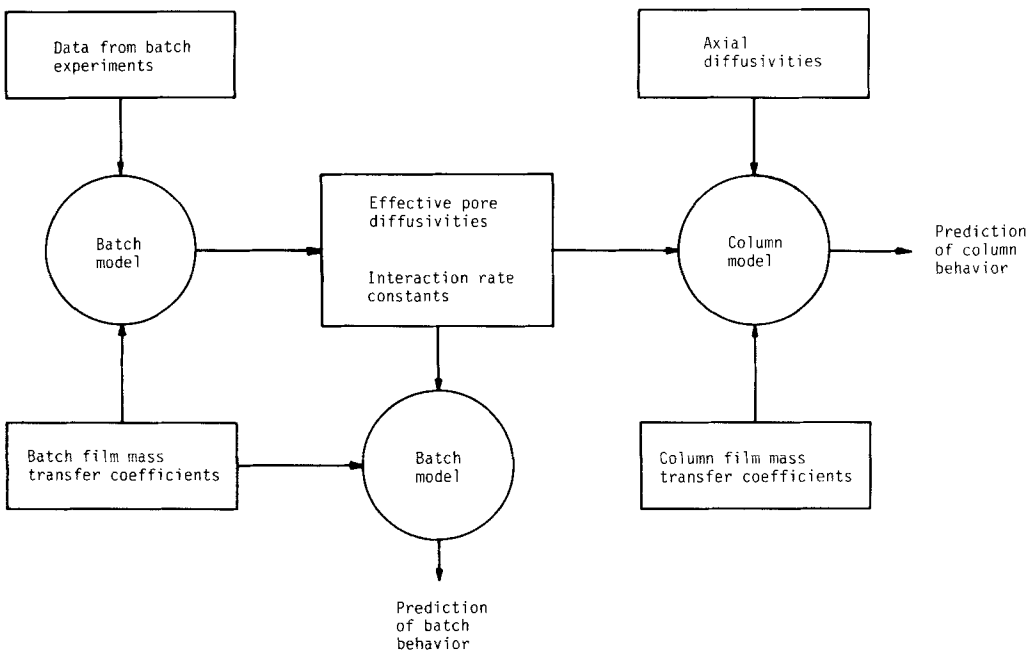

Figure 1. Information flow of data used in batch and column models to predict behavior of biospecific adsorption.

Table 1. Parameter Values for Adsorption of β-galactosidase onto Anti-β-galactosidase Immobilized on Porous Silica, Batch System

$C_{dol} = 1.58 \times 10^{-2}$ mg/cm^3	$k_2 = 1.2 \times 10^{-6}$ s^{-1}**
$C_T = 2.2$ mg/cm^3	$R_o = 7.5 \times 10^{-3}$ cm
$K_{Dl} = 2.2 \times 10^{-4}$ mg/cm^3	$\epsilon = 0.985$
$K_{Al} = 4.54 \times 10^3$ cm^3/mg	$\epsilon_p = 0.5$***
$K_{fl} = 5.84 \times 10^{-4}$ cm/s*	Molec. wt. = 464,000 g/mol
$k_1 = 5.5 \times 10^{-3}$ cm^3/mg · s**	$V = 101.5$ cm^3**

*Estimated value (Geankoplis, 1983, p. 440)
**Chase's model (1984b)
***Chase, H.A., private communication (1985)

Table 2. Estimated Parameter Values for Models Used for Curves 2, 3, 4, Figure 2

Curve 2, Second-order reversible interaction
$k_{1,1} = 0.0235$ cm^3/mg · s
$D_{pl} = 6.9 \times 10^{-8}$ cm^2/s

Curve 3, Langmuir isotherm
$K_{fl} = 0.352 \times 10^{-4}$ cm/s
$D_{pl} = 14.3 \times 10^{-8}$ cm^2/s

Curve 4, Langmuir isotherm
$D_{pl} = 3.40 \times 10^{-8}$ cm^2/s
$K_{fl} = 5.84 \times 10^{-4}$ cm/s (from correlation)

Langmuir expression
$C_{sl} = K_{Al} C_T C_{pl}/(1 + K_{Al} C_{pl})$

work when a second-order reversible rate expression is used to describe the adsorbate-ligand interaction, curve *2*. The model of Chase, curve *1*, predicts a lower adsorption rate during the initial part of the adsorption stage and a higher rate at later times. It is also interesting to note that a larger value of the rate constant $k_{1,1}$ is estimated by the pore-diffusion model with the second-order reversible interaction rate, Table 2, when compared with the value of the same parameter estimated by Chase's model, Table 1. This latter observation indicates that the rate constants in Chase's model are parameters that lump the effects of the interaction mechanisms between the adsorbate and the ligand together with the mass transfer mechanisms characterizing the transport of solutes, since the model of Chase ignores mass transfer resistances.

It is also observed in Figure 2 that when the Langmuir isotherm is used and both D_{pl} and K_{fl} are estimated simultaneously, curve *3*, a fairly good agreement is obtained between theory and experiment. However, the estimated value of K_{fl} is about 17 times smaller than that calculated from a correlation in the literature. This result may imply that existing literature correlations do not apply to macromolecules of very high molecular weight

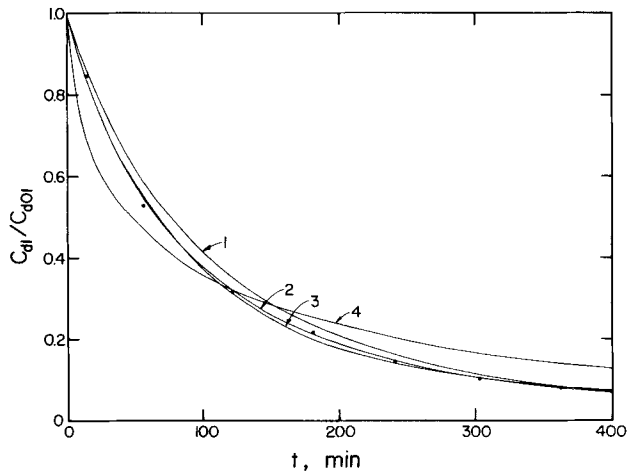

Figure 2. Time variation of β-galactosidase concentration in bulk fluid phase of finite bath.
● Experimental data (Chase, 1984b)
1 Predictions, Chase (1984b) model
2 Predictions, pore-diffusion model, interaction rate given by second-order reversible expression (Eq. 11)
3 Predictions, pore-diffusion model, local equilibrium between adsorbate and adsorbate-ligand complex at each point in pore (Langmuir isotherm, Table 2); D_{pl} and K_{fl} estimated simultaneously
4 As curve 3; D_{pl} estimated, K_{fl} calculated from a correlation

and that new correlations should be developed. On the other hand, one may suggest that the model of curve *3* may not accurately describe the adsorption stage and, therefore, the estimated values for K_{fl} and D_{pl} may simply represent curve-fitted values. It is apparent that more sets of experimental data are needed in order to discriminate between various models (Froment and Hosten, 1981). It is hoped that Chase and others doing experimental work in biospecific adsorption will provide in the future adequate data so that more appropriate model discrimination and parameter estimation procedures may be used.

If the vale of K_{fl} obtained by the correlation in the literature is a good estimate of K_{fl}, then there is a large discrepancy between the experimental data and the predictions of the model used in curve *4*. Computer experiments performed by using the model in curves *3* and *4* and varying the values of the parameters K_{fl} and D_{pl} within the ranges defined by the data in Tables 1 and 2, suggest that both mass transfer resistances have a significant influence on the quantitative behavior of biospecific adsorption, but that the effect of the pore diffusion resistance is larger than that of the film mass transfer resistance. Our simulations indicate that in order to predict accurately the experimental results in Figure 2, the model must account for the film mass transfer and pore diffusion resistances as well as for the interaction mechanism of the adsorbate-ligand complex; this is clearly indicated in curve *2*. It is also worth noting that the pore diffusivities reported in Table 2 have meaningful values because the corresponding diffusivity of β-galactosidase in free solution reported in the literature (Sorber, 1968) or estimated by a correlation (Geankoplis, 1983, p. 395) has values between 3.12×10^{-7} and 3.90×10^{-7} cm^2/s. These free solution diffusivities and the pore diffusivities in Table 2 suggest that the tortuosity of the porous adsorbent can have values in the range of 2.26 to 2.83 for curve *2*, in the range of 1.10 to 1.36 for curve *3*, and in the range of 4.59 to 5.74 for curve *4*. Since curve *2* provides the best agreement between theory and experiment, it is thought that the proper value of the tortuosity is between 2.26 and 2.83. Also, the values of Po_l and Sh_{pl}, which can be calculated from the estimated parameters given in Table 2, are 481 cm^3/mg and 254, respectively, for the system described by curve *2*. For the systems described by curves *3* and *4*, the value of Sh_{pl} is 7.4 and 515, respectively.

In the following paragraphs the dynamic behavior of single-component biospecific adsorption in a finite bath is studied for different parameter values of the model equations presented in this work. The values of the parameters used in the computer

experiments that produced the data in Figures 3–8 are given in Table 3.

In Figure 3 the dimensionless bulk phase concentration is shown as a function of time, τ, when the interaction between the adsorbate and the ligand is described by a second-order reversible expression, Eq. 11, and with Sh_{pl} and Po_l as parameters. It should be noted that as $Po_l \rightarrow \infty$, the results predicted by the second-order reversible interaction model would approach those obtained by the local-equilibrium model. Several preliminary computer experiments showed that for values of Po_l larger than about 10^6 cm^3/mg, the results are indeed very close to the data obtained from the model that assumes local equilibrium between the adsorbate and the adsorbate-ligand complex at each point in the pores of the particles. These findings imply that values of Po_l equal to 0.1 and 1,000 cm^3/mg, as used in Figure 3, would correspond to slow and fast rates of interaction relative to the rates of mass transfer in the pores.

In Figure 3 it is seen that for $Po_l = 0.1$ cm^3/mg the adsorption rates are fairly close for both $Sh_{pl} = 0.1$ and $Sh_{pl} = 100$. The results imply that for this low value of Po_l the adsorbate-ligand interaction is the major rate-controlling step, and that when the value of Sh_{pl} increases 1,000 times the adsorption rate increases only slightly. For a constant Sherwood number of 0.1 and when the value of Po_l increases from 0.1 to 1 cm^3/mg, the rate of adsorption increases significantly. It was also found that for $Sh_{pl} = 0.1$ and $Po_l = 1{,}000$ cm^3/mg the adsorption rate shown in Figure 3 is fairly close to that observed for the local-equilibrium model with $Sh_{pl} = 0.1$ (Arve, 1986). It may therefore be concluded that for $Sh_{pl} = 0.1$ and when Po_l varies from 0.1 to 1,000 cm^3/mg, the adsorption process changes from being mostly interaction rate-limited to being mostly mass-transfer rate limited. It is also seen in Figure 3 that for a value of $Sh_{pl} = 100$, when Po_l varies from 0.1 to 100 cm^3/mg there is a very large increase in the rate of adsorption.

Computer simulations were also carried out for the same values of Sh_{pl} and Po_l as those shown in Figure 3 but with $K_{Dl} = 10^{-8}$ mg/cm^3, which would represent a stronger binding between the adsorbate and the ligand. It was found that the concentration in the adsorbed phase is larger compared to the case with $K_{Dl} = 10^{-4}$ mg/cm^3 since a lower value of K_{Dl} shifts the concentration distribution toward the adsorbate-ligand complex. Due to this shift in the concentration distribution between unbound adsorbate and the adsorbate-ligand complex, the adsorption rate was observed to be slightly larger for the lower value of K_{Dl}.

In Figure 4 the dimensionless concentration profiles of the unbound adsorbate and adsorbate-ligand complex within the adsorbent particles predicted by the second-order reversible interaction model are shown for different dimensionless times. The values of Sh_{pl} and Po_l are equal to 100 and 100 cm^3/mg,

Table 3. Parameter Values Used in Model Simulations, Figures 3–8

$C_{dol} = 1.58 \times 10^{-2}$ mg/cm^3*	$R_o = 5 \times 10^{-3}$ cm
$C_T = 2.2$ mg/cm^3*	$\epsilon = 0.985$*
$K_{Dl} = 10^{-4} - 10^{-8}$ mg/cm^3	$\epsilon_p = 0.46$**
$\frac{\text{Amt. adsorbate}}{\text{Amt. avail. ligand}} = 0.478$	$V = 101.5$ cm^3*

*Chase (1984b)
**Katoh et al. (1978)

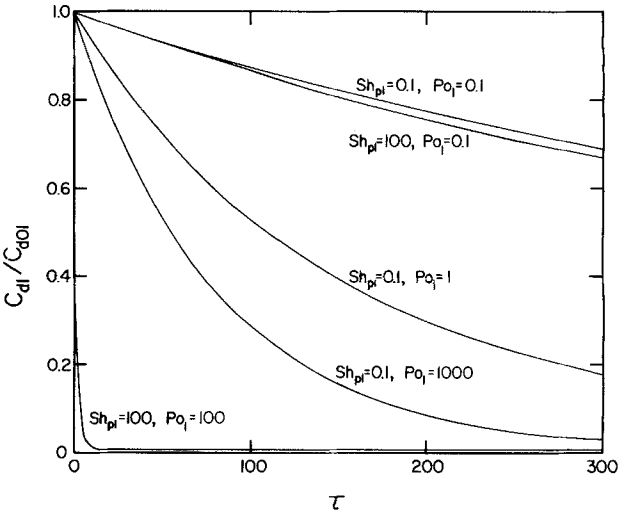

Figure 3. Time variation of adsorbate concentration in bulk fluid phase of finite bath for various values of Sherwood number and Porath parameter.
Second-order reversible interaction rate (Eq. 11), $K_{Dl} = 10^{-4}$ mg/cm^3

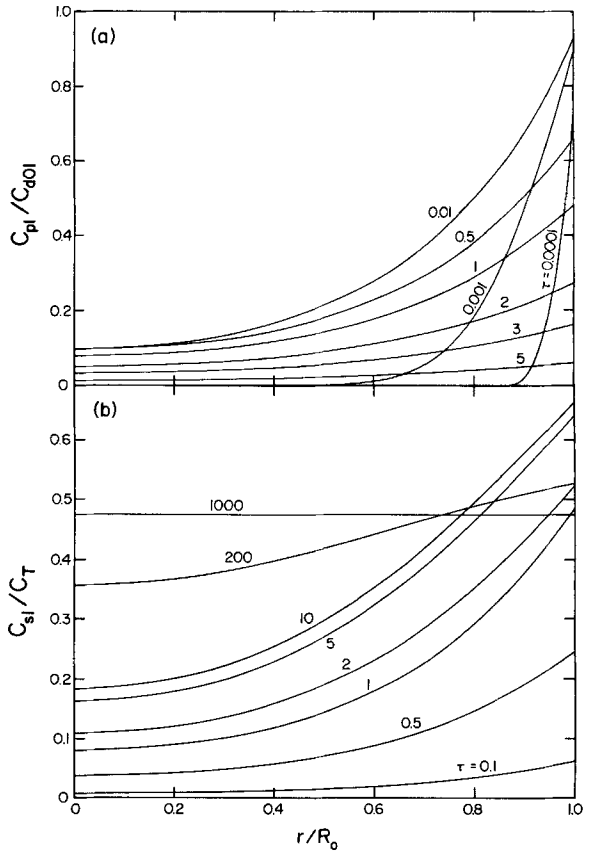

Figure 4. Concentration profiles in adsorbent for various times, τ.
Second-order reversible interaction rate (Eq. 11), $K_{Dl} = 10^{-4}$ mg/cm^3; $Sh_{pl} = 100$; $Po_l = 100$ cm^3/mg
(a) Concentration of adsorbate in fluid of pore
(b) Concentration of adsorbate-ligand complex

respectively, and these values are of the same order of magnitude as those obtained in the simple parameter-estimation study presented above—see Figure 2 and Table 2. In Figure 4a it is seen that the concentration of unbound adsorbate at the outer part of the particles increases fairly rapidly, goes through a maximum value, and then decreases toward the equilibrium value. It is also observed that the maximum concentration at the external surface of the particles ($r/R_o = 1$) is close to the initial concentration in the finite bath.

In Figure 4b the concentration profiles of the adsorbate-ligand complex are presented, and it is seen that the dynamic behavior is somewhat similar to that of the unbound adsorbate shown in Figure 4a. However, a distinct time lag is observed in the accumulation of the adsorbate-ligand complex; this results from the finite rate of interaction. It is also observed in Figure 4b that a fairly long time is required to reach equilibrium conditions.

Results from several computer experiments (Arve, 1986) have shown that the dynamic behavior of systems with small values of the Porath parameter are similar to each other, and almost independent of the value of K_{D1}. However, when Po_1 has a large value the results are quite different for different values of K_{D1}. It was observed that for fairly weak adsorbate-ligand bindings ($K_{D1} = 10^{-4}$ mg/cm^3), the concentrations both in the fluid and solid phases reach equilibrium at moderately short dimensionless times, whereas for strong binding ($K_{D1} = 10^{-8}$ mg/cm^3) the concentrations reach equilibrium only at extremely large times, τ. This may be of great importance for both the wash and elution stages. First, a low value of K_{D1} would imply that less material is lost during the wash stage. Second, a stronger eluent may have to be used during the elution stage to ensure a satisfactory recovery of the adsorbate. Thirdly, a low value of K_{D1} may cause the adsorbate to adsorb primarily at the outer parts of the particle. This may imply that ligands immobilized in the interior parts of the particle are not effectively utilized, which in turn may suggest that a radial distribution of the ligands may be desirable where only the outer parts of the solid support matrix are covered with ligands.

In Figures 5 and 6 results obtained from the solution of the multivalent interaction model, Eq. 18, with $z = 2$ are shown for different parameter values of Sh_{p1}, $Po_{1,1}$, and $Po_{1,2}$. In all cases

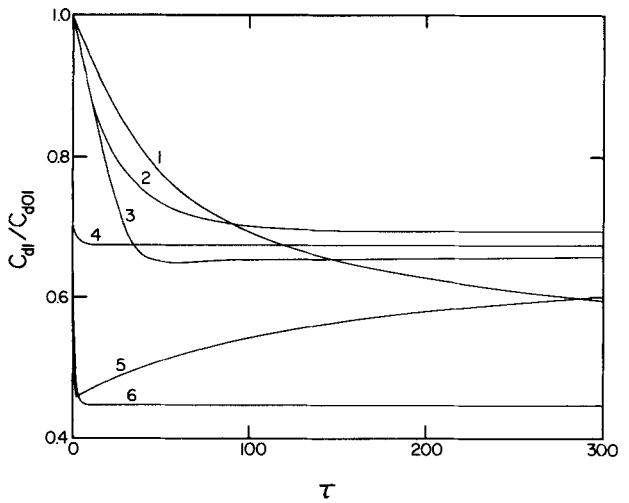

Figure 5. Time variation of bivalent adsorbate concentration in bulk fluid phase of finite bath for various parameter values.

Curve	Sh_p1	$Po_{1,1}$ cm^3/mg	$Po_{1,2}$	$K_{D1,1}$ mg/cm^3	$K_{D1,2}$ mg/cm^3
1	0.1	1	2.2	10^{-4}	0.1
2	100	1	2.2	10^{-4}	10^{-4}
3	0.1	1,000	2.2	10^{-4}	10^{-4}
4	100	1,000	2,200	10^{-4}	10^{-4}
5	100	1,000	2.2	10^{-4}	10^{-4}
6	100	1,000	2,200	10^{-4}	0.1

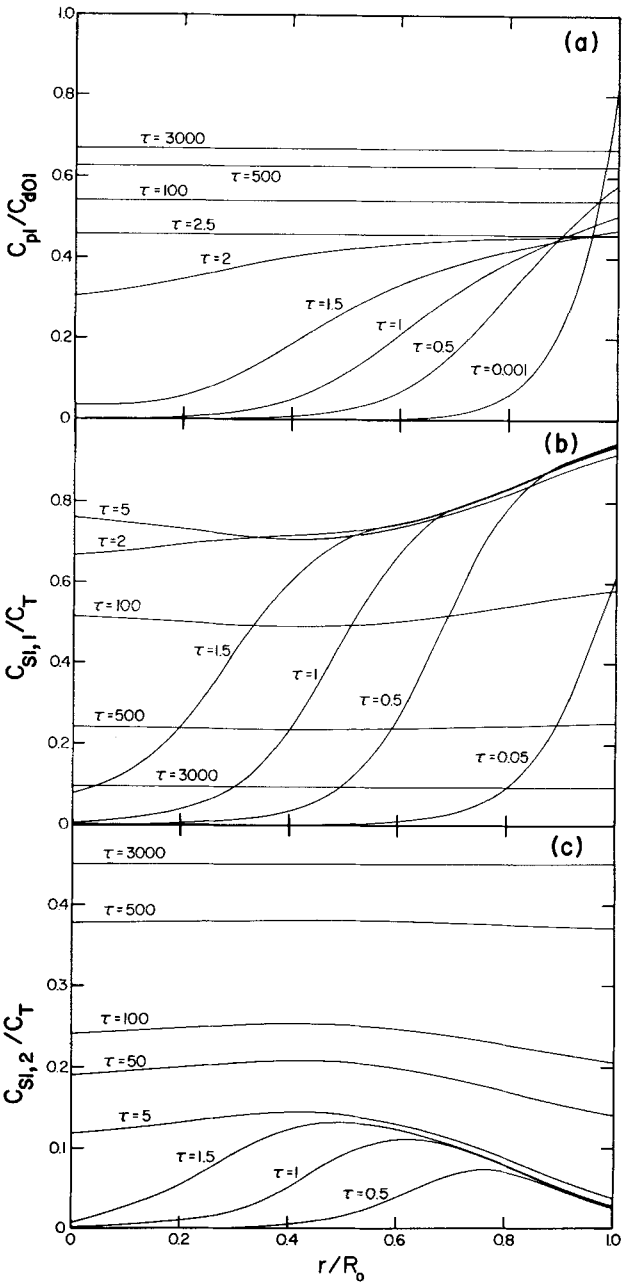

Figure 6. Profiles of bivalent adsorbate concentration in adsorbent for various times, τ.

$Sh_{p1} = 100$; $K_{D1,1} = 10^{-4}$ mg/cm^3; $K_{D1,2} = 10^{-4}$ mg/cm^3; $Po_{1,1} = 1{,}000$ cm^3/mg; $Po_{1,2} = 2.2$

(a) Concentration of adsorbate in fluid of pore
(b) Concentration of one-site interaction complex
(c) Concentration of two-site interaction complex

$K_{D1,1} = 10^{-4}$ mg/cm^3 and $K_{D1,2}$ ranges from 10^{-4} to 0.1 mg/cm^3. It should be noted that the ratio of the total amount of adsorbate to the total amount of ligand is taken to be equal to 1.7 in this system and was so chosen in order to show clearly the effect of the bivalent interaction.

Curves *2–5* in Figure 5 represent systems with $K_{D1,1} = K_{D1,2} = 10^{-4}$ mg/cm^3 while curves *1* and *6* represent cases with $K_{D1,1} = 10^{-4}$ mg/cm^3 and $K_{D1,2} = 0.1$ mg/cm^3. It is observed that the capacity of the adsorbent decreases with decreasing values of $K_{D1,2}$. At equilibrium, the capacity is approximately 50% less when $K_{D1,2} = 10^{-4}$ mg/cm^3 compared with the case where $K_{D1,2} = 0.1$ mg/cm^3. This phenomenon occurs because a lower value of $K_{D1,2}$ means that the equilibrium distribution between the one-site and two-site interaction of the adsorbate is shifted toward the interaction with two sites. Hence, as a larger amount of the adsorbates form adsorption complexes with two sites and ocupy two ligands, the capacity of the adsorbent will decrease. However, if the ratio between the total amount of adsorbate to the total amount of ligand is less than 0.5, the effect of decreasing capacity with decreasing values of $K_{D1,2}$ will not be as significant in the initial stage of the adsorption process as is the case when this ratio is 1.7. In fact, at equilibrium the value of $K_{D1,2}$ would not influence the capacity since most of the adsorbate would have been adsorbed (even if most adsorbate-ligand complexes involve two-site interactions).

A very interesting result is observed in curve *5*, which was obtained for $Sh_{p1} = 100$, $Po_{1,1} = 1{,}000$ cm^3/mg, and $Po_{1,2} = 2.2$. It is seen that the bulk phase concentration decreases very rapidly to a minimum value and then starts to increase toward the equilibrium value; this suggests that material is being desorbed from the adsorbent. The result indicates that there is competition for the available ligands between adsorbate molecules forming complexes with one-site interactions and those molecules establishing complexes with two-site interactions. Because of the relatively large value of $Po_{1,1}$ compared with $Po_{1,2}$, during the initial stage most of the adsorbates will attach themselves with one site only. But as time progresses, the favored attachment with two sites (low value of $K_{D1,2}$) will force material to desorb. A similar behavior is observed in curve *3* but the minimum concentration is not as small as in the previous case; this is due to the lower value of Sh_{p1}. From these observations it may be concluded that desorption of the complex with one-site interaction may be expected during the adsorption process when the two-site attachment is favored (low value of $K_{D1,2}$) and $Po_{1,1}$ is larger than $Po_{1,2}$. It should be noted that no desorption was observed for the case with $K_{D1,2} = 0.1$ mg/cm^3.

Curve *1* in Figure 5 shows that a much lower adsorption rate is obtained with low values of Sh_{p1}, $Po_{1,1}$ and $Po_{1,2}$ compared to high values for these parameters, curve *6*, as is expected. Cases with low values of $Po_{1,1}$, curve *2*, indicated that the rate of formation of the complex with one-site interaction was the major rate-limiting step, and the adsorption rates changed only slightly when both Sh_{p1} and $Po_{1,2}$ were changed by several orders of magnitude. It is also seen in Figure 5 that very large adsorption rates are obtained when $Sh_{p1} = 100$, $Po_{1,1} = 1{,}000$ cm^3/mg, and $Po_{1,2} = 2{,}200$ for both $K_{D1,2} = 10^{-4}$ mg/cm^3 (curve *4*) and $K_{D1,2} = 0.1$ mg/cm^3 (curve *6*).

In Figure 6 the concentration profiles of (a) unbound adsorbate, (b) the adsorption complex with one-site interaction, and (c) the adsorption complex with two-site interaction, are shown for $K_{D1,1} = K_{D1,2} = 10^{-4}$ mg/cm^3, $Sh_{p1} = 100$, $Po_{1,1} = 1{,}000$ cm^3/mg, and $Po_{1,2} = 2.2$. The concentration profile in the pore fluid displays a dynamic behavior similar to that observed previously in this work for cases with high values of Sh_{p1} and relatively fast interaction rates: the concentration becomes fairly high close to the external surface of the particle and a large concentration gradient is established within the particle. As time progresses, the concentration at the outer parts of the particle decreases, while material continues to be transported toward the center of the particle. At about $\tau = 2.5$ an almost uniform concentration distribution is reached. But contrary to all the previous cases studied, the concentration of unbound adsorbate starts to increase again after being almost constant for a certain period of time, and the equilibrium concentration is reached only at very large dimensionless times τ.

Because of the large value of $Po_{1,1}$ compared to $Po_{1,2}$, it is seen in Figure 6b that the dynamic behavior of the concentration profiles of the one-site interaction complex is similar to that of the unbound adsorbate during the beginning of the adsorption process. A concentration profile with significant amounts of one-site interaction complex at all radial positions is obtained at about $\tau = 5$, after which the concentration steadily decreases to the equilibrium value of 0.1. This phenomenon is due to the fact that as the concentration of the one-site interaction complex increases, so does the interaction rate for the formation of the two-site interaction complex; and since the dissociation constant for the two-site interaction complex is so low, 10^{-4} mg/cm^3, the adsorption of the two-site interaction complex will be favored. As a consequence of the competition for the ligands, some material will desorb and the concentration of the one-site interaction complex will decrease.

In Figure 6c the concentration profiles of the two-site interaction complex are shown. It is seen that the concentration reaches a maximum value inside the particles, and this maximum concentration moves towards the center of the particles as time progresses. Close to the end of the adsorption process the distribution of the two-site interaction complex has become almost uniform within the particle. The reason for the occurrence of this interior maximum concentration is that the concentration of the one-site interaction complex, Figure 6b, increases rapidly at the outer parts of the particle and reduces the number of vacant ligands with which a one-site interaction complex can attach to a ligand with its second site. Because of mass transfer resistance within the particle, there is a higher concentration of vacant ligands toward the center of the particle, and thus the concentration of the two-site interaction complex increases more rapidly in this region of the particle.

It should be noted that while multivalent binding may increase the strength of the adsorbate-ligand binding, it may be at the expense of lost capacity of the adsorbent since one adsorbate molecule will occupy two or more ligands. It may therefore, in certain cases, be desirable to terminate the adsorption stage before the concentration of the two-site interaction complex has increased to a large value. A small concentration of the two-site interaction complex may also be desirable during the elution stage when effective elution methods for the dissociation of the two-site interaction complex are considered. Elution methods that are too harsh may decrease the biological activity of the adsorbate, thus making the product to be of less commercial interest. On the other hand, a strong binding due to multivalent

interactions may be favorable in cases that require long periods of washing, since a strong binding will minimize the losses of the material of interest during the wash stage.

Wash stage

In this work, washing with weak buffer solutions is considered; therefore, it is assumed that the values of the model parameters used in the analysis of the adsorption stage will not change significantly during the wash stage. Thus the data given in Table 3 are applicable to the wash stage as well, except for the parameter C_{do1}, which is equal to zero at the start of the wash stage. It should also be noted that the ratio of the total amount of adsorbate to the total amount of available ligand will be different in the wash stage if the total amount of adsorbate at the start of the adsorption stage has not been adsorbed onto the ligands when the adsorption stage is terminated.

The adsorption stage of biospecific separation in a finite bath will in most cases be terminated when the bulk phase concentration of the species of interest dips below a certain specified level. This concentration level should be very small in order to ensure a satisfactory recovery of the desired solute (product). In the present work it is arbitrarily taken to terminate the adsorption stage when the concentration of the adsorbate of interest in the bulk fluid phase has decreased to about 1% of the initial concentration level. The concentration distributions of unbound adsorbate and adsorbate-ligand complex within the pores of the adsorbent particles at the time when the bulk fluid phase concentration of the adsorbate has decreased to about 1% of the initial concentration level, provide the initial conditions for the adsorbates ($i = 1, 2, \ldots, m$) in the wash stage. To obtain the initial conditions in the wash stage for the nonadsorbed contaminants ($i = \ell + 1, \ldots, n$), the appropriate material balance equations (Eqs. 1 and 3b with $\delta = 0$) have to be solved for each contaminant. In this work only one contaminant is considered. Its model expressions for the adsorption and wash stages were solved with $\delta = 0$ and for the parameter values shown in Table 4. In most cases it was found that the concentration of the contaminant reached closely its equilibrium value before the adsorption stage was terminated (Arve, 1986).

In Figure 7 the time variation of the dimensionless bulk phase concentrations of the adsorbate of interest (curves *1–7*) and of the contaminant (curves *8* and *9*) during the wash stage are shown. Curves *1* and *2* display a very interesting result in that the bulk phase concentration initially increases quite fast, passes through a maximum value, and then decreases toward the equilibrium value of about 0.0053. This phenomenon occurs for these two systems because when the adsorption stage is terminated, fairly large concentration differences still exist within the pores of the particles, and the concentrations of the unbound adsorbate and adsorbate-ligand complex are, at the outer parts of the particles, larger than the concentrations that would be established if the adsorption stage had been allowed to reach its

Table 4. Parameter Values for Contaminant

$C_{do2} = 1.58 \times 10^{-4}$ to 1.58 mg/cm^3*	$Sh_{p2} = 0.01$ to 100
$C_{do2} = 0.0$ mg/cm^3**	$D_{pR2} = 0.1$ to 1

Concentration of contaminant in bath:
*at $\tau = 0$; **at $\tau_w = 0$

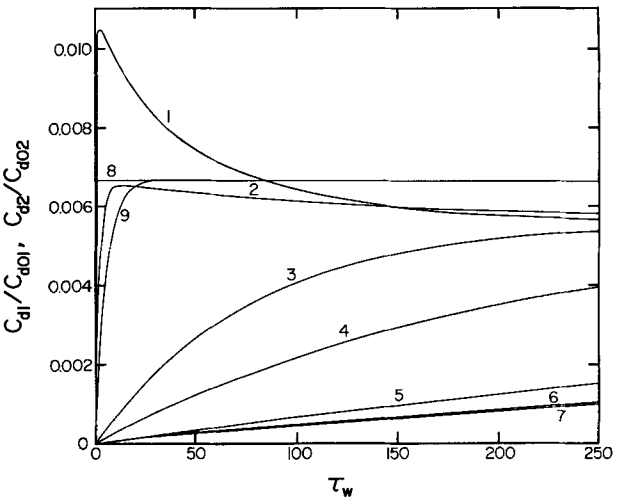

Figure 7. Time variation of adsorbate and contaminant concentrations in bulk fluid phase of finite bath during wash stage.

C_{do1}, adsorbate concentration at beginning of adsorption stage
C_{do2}, contaminant concentration at beginning of adsorption stage

Curve	Component; Model*	Sh_{p1}	Sh_{p2}	Po_1 cm^3/mg	K_{D1} mg/cm^3
1	Ads; Local	100	—	—	10^{-4}
2	Ads; 2d or.	100	—	100	10^{-4}
3	Ads; 2d or.	0.1	—	1,000	10^{-4}
4	Ads; 2d or.	0.1	—	1	10^{-4}
5	Ads; Local	0.01	—	—	10^{-4}
6	Ads; 2d or.	100	—	0.1	10^{-4}
7	Ads; 2d or.	0.1	—	0.1	10^{-4}
8	Con —	—	100	—	—
9	Con —	—	0.01	—	—

*Ads, adsorbate; Con, contaminant
Local, local equilibrium between adsorbate and adsorbate-ligand complex at each point in pore (Langmuir isotherm, Table 2)
2d or., second-order reversible interaction rate (Eq. 11)

equilibrium state. When the wash stage starts, the adsorbate because of its large Sherwood number will rapidly diffuse out of the particles and into the bulk fluid phase where the concentration of the adsorbate will increase to a level above the equilibrium value. After a certain period of time a concentration gradient is established that results in the transport of adsorbate from the bulk phase into the adsorbent particles in a similar manner as during the adsorption stage. For the cases studied in this work, the largest amount of product loss (adsorbate leaving the particles and entering into the bulk fluid phase) during the wash stage occurs for the system where the adsorbate and adsorbate-ligand complex are at equilibrium, $Sh_{p1} = 100$, and $\tau_w = 2.5$. The loss of product at this point in time would amount to about 1.05% of the total amount of product in the particles at the beginning of the wash stage. However, if the adsorbate concentration is allowed to approach closely its equilibrium value during the wash stage, then the loss of product would be only about 0.56% of the initial total amount. It would therefore seem appropriate in certain cases to prolong the wash stage in order to minimize the loss of product. The increased loss of product that would occur during the overshoot of the adsorbate concentration in the bulk phase may be prevented by allowing the adsorption stage to continue until the adsorbate concentration has more closely approached its equilibrium value, since at this point the

concentration profiles in the pores of the particles would be almost uniform.

Curves *3*, *4*, and *7* in Figure 7 show the bulk phase concentration of the adsorbate when the adsorbate-ligand interaction is described by a second-order reversible rate expression, Sh_{p1} = 0.1, and for values of the Porath parameter equal to 1,000, 1, and 0.1 cm^3/mg, respectively. It is observed that a low value of the Porath parameter significantly reduces the rate at which product is lost during the wash stage. A comparison of the results in curves *5*, *6*, and *7* suggests that for the systems with Po_1 = 0.1 cm^3/mg, the rates at which adsorbate is lost during the wash stage are smaller than those of the system whose adsorbate is at equilibrium with the adsorbate-ligand complex at each point in the pore and Sh_{p1} = 0.01. It is also seen from curves *6* and *7* that the value of the Sherwood number has a very small effect on the rate of loss of adsorbate from the particles during the wash stage when Po_1 = 0.1 cm^3/mg.

Curves *8* and *9* in Figure 7 show the concentration of the contaminant in the finite bath during the wash stage. It is observed from curve *8* (Sh_{p2} = 100) that initially the washout rate of the contaminant is approximately the same as that of the adsorbate of interest under the conditions in curve *1*. However, no overshoot is observed for the contaminant since its concentration in the particles had approached closely the equilibrium value during the adsorption stage. It is also seen that if the wash stage is terminated when the concentration of the contaminant reaches its maximum level of about 0.0067 in the finite bath, then the loss of prduct would be quite small for most systems studied in this work. Only in the case represented by curve *1* may the amount of lost product be significant. On the other hand, if the value of the Sherwood number for the contaminant is equal to 0.01 (curve *9*) and the wash stage is discontinued when the concentration of the contaminant has approached closely its equilibrium value of 0.0067, then the loss of product may have to be considered for all the systems examined in this work. In fact, alternative operating conditions for the wash stage may be necessary in order to keep the loss of product within acceptable levels. It may, in some cases, be advantageous to choose a different wash buffer solution or to operate at a lower temperature in order to decrease the value of the dissociation constant of the adsorbate-ligand complex, and this would reduce the amount of product lost during the wash stage. For the systems with a dissociation constant equal to 10^{-8} mg/cm^3, the maximum loss of product in the wash stage did not exceed 0.01% of the total amount of adsorbate in the particles at the beginning of the wash stage.

The time duration of the wash stage is primarily dictated by the required product purity, which will have to be determined individually for each product. For washing in a finite bath it may in certain cases be necessary to use more than one wash in order to reduce the concentration of a contaminant to a certain specified level, and thereby satisfy the product purity requirements. In the event that the wash stage for a certain system involves multiple washes and the total time duration of the wash stage is long, then it may be necessary to discontinue the wash stage before the product purity requirements are met, in order not to lose unacceptable amounts of the product.

As an example, a "difficult" case is considered where the amount of the contaminant at the beginning of the adsorption stage is 158 mg, that is 100 times larger than the amount of the adsorbate of interest (product). The value of Sh_{p2} is equal to 0.01 and D_{pR2} = 0.1, and it is taken that the duration of the adsorption stage is long enough for the contaminant concentration in the pores to reach its equilibrium value. The product purity is required to be 99.9999% which means that after the elution stage only 10^{-6} mg of contaminant is allowed in 1.0 mg of eluted product solution. In this particular case, the total amount of contaminant in the adsorbent particles has to be reduced at least to 1.56×10^{-6} mg during the wash stage, since at the end of the adsorption stage 1.56 mg of product have been biospecifically adsorbed. We say above that the amount of the contaminant has to be reduced at the least to 1.56×10^{-6} mg because during the wash stage some of the adsorbed product is lost by leaving the adsorbent particles and entering the bulk wash solution in the bath. This high product purity requirement is characteristic of pharmaceutical products (Janson and Nystrom, 1985).

At the end of the adsorption stage the adsorbent particles of the system of interest are resuspended in a wash buffer solution, and the volume of the bath is taken to be the same as that of the bath used in the adsorption stage, Table 3. In this example, the total amount of contaminant in the pores of the adsorbent particles is 1.06 mg at the end of the adsorption stage. In Table 5 the number of washes and overall wash time required to reduce the amount of the contaminant from 1.06 mg to 1.56×10^{-6} mg are given for four different systems. In system 1, each wash was terminated when the concentration of the contaminant in the bath had reached 85% of its equilibrium value. It should be noted that the equilibrium concentration has a different value for each wash. For systems 2, 3, and 4, each wash was terminated when the concentration of the contaminant in the bath had reached 90, 95, and 99% of its equilibrium value, respectively.

It is observed in Table 5 that the number of washes varies between eight (system 1) and four (system 4), and that although the required overall wash time does not vary substantially for systems 1, 2, and 3, the wash time of system 4 is significantly longer. It should be noted that the wash times reported in Table 5 include only the actual washing of the adsorbent particles and do not account for the times required to drain the bath after each wash and resuspend the particles in a fresh wash buffer solution. Because of the long duration of the wash stage for the systems studied in this example, one has to consider the total amount of product lost during the wash stage. With reference to Figure 7 it is apparent that the largest losses of product will occur in systems where the Sherwood number for the product is high and the interaction rate of the adsorbate and ligand is very large or infinitely fast (curves *1* and *2* in Figure 7). In the present example, Tables 5 and 6, the adsorbate of interest (product) is considered to be at equilibrium with the adsorbate-ligand

Table 5. Washing Required to Reduce Contaminant from 1.06 mg to 1.56×10^{-6} mg

System	Contam. Conc. at End Each Wash % Equilib. Value	No. of Washes	Time in Wash Stage, τ_w
1	85	8	770
2	90	7	775
3	95	5	785
4	99	4	840

complex at each point in the pore (Langmuir isotherm in Table 2), $Sh_{p1} = 100$, and $K_{D1} = 10^{-4}$ mg/cm^3. In Table 6, the total amount of product lost during the wash stage for the systems shown in Table 5 is reported. Also, the percentage of product lost relative to the total amount of 1.56 mg of product is given in Table 6. It is observed that the smallest loss of product occurs in the system with the least number of washes (system 4), although the time required for the wash stage of this system is the longest. It is apparent from the data presented in Tables 5 and 6 that the procedure selected to be used in the wash stage will involve a compromise between the number of washes required to achieve a given product purity and the amount of product that would be accepted to be lost during the required overall wash time.

In Figure 8 the time variation of the bulk phase concentration of a bivalent adsorbate during the wash stage is shown. It is observed from curves *1–4* that a fairly large overshoot in the concentration of the product (adsorbate) may occur when $Sh_{p1} = 100$ and $Po_{1,1} = 1{,}000$ cm^3/mg. This overshoot is partly due to the same phenomenon that was discussed for the monovalent adsorbate's dynamic behavior shown by curve *1* of Figure 7; that is, there exists a fairly large concentration gradient in the pores of the particles at the start of the wash stage (end of the adsorption stage), and because of the large value of Sh_{p1}, absorbate will rapidly transfer out of the adsorbent particles and into the bulk fluid phase. Furthermore, in a system involving bivalent components the adsorbate may be displaced from the ligands in the outer part of the particles because of competition between molecules forming one-site and two-site interaction complexes. The displaced adsorbate may contribute significantly to the mass flux of product leaving the particles, and may lead to a very large overshoot in the concentration of the adsorbate (relative to its equilibrium value) in the finite bath, as is seen in curve *3* of Figure 8. From curves *1* and *2* it is observed that the overshoot is of similar size for $Po_{1,2} = 2.2$ and $Po_{1,2} = 2{,}200$ when $K_{D1,2} = 0.1$ mg/cm^3. However, by comparing curves *3* and *4* it is seen that the magnitude of the overshoot is much larger for $Po_{1,2} = 2.2$ than $Po_{1,2} = 2{,}200$ when $K_{D1,2} = 10^{-4}$ mg/cm^3. This occurs because for the case where $Po_{1,2} = 2.2$, the concentration of the two-site interaction complex is lower in the outer part of the particles at the beginning of the wash stage than the concentration of the same complex with $Po_{1,2} = 2{,}200$. Furthermore, the ligands are almost completely occupied in the outer part of the particles, and since the two-site interaction is favored, more adsorbate is displaced in this region of the particles for the system having the lower value of $Po_{1,2}$.

In curves *5–8* in Figure 8 it is shown clearly that for a low value of the Sherwood number ($Sh_{p1} = 0.1$), the washout rate of adsorbate is almost independent of the value of $Po_{1,2}$. The results of curves *9* and *10* show the concentration of the contaminant in the finite bath during the wash stage. The dynamic behavior of the contaminant is identical to that shown in curves *8* and *9* of Figure 7. The results in Figure 8 also show that in general less product will be lost during the wash stage for a system having a lower value of $K_{D1,2}$. However, the loss of product is greatly dependent upon the time at which the wash stage is terminated, as can be clearly seen in Figure 8. The concentration profiles within the adsorbent particles are presented in Arve (1986).

Finally it is worth noting that the results obtained through the analysis of the wash stage provide the initial conditions of the elution stage of biospecific separations.

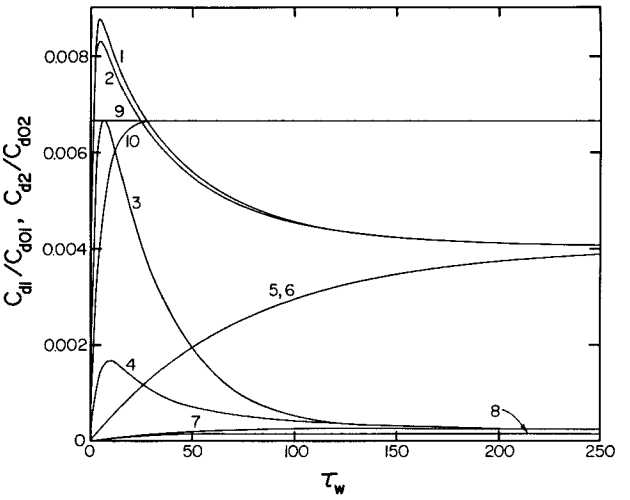

Figure 8. Time variation of bivalent adsorbate and contaminant concentrations in bulk fluid phase of finite bath during wash stage.

C_{do1}, adsorbate concentration at beginning of adsorption stage
C_{do2}, contaminant concentration at beginning of adsorption stage

Curve	Component*	Sh_{p1}	Sh_{p2}	$Po_{1,1}$ cm^3/mg	$Po_{1,2}$	$K_{D1,1}$ mg/cm^3	$K_{D1,2}$ mg/cm^3
1	Ads	100	—	1,000	2.2	10^{-4}	0.1
2	Ads	100	—	1,000	2,200	10^{-4}	0.1
3	Ads	100	—	1,000	2.2	10^{-4}	10^{-4}
4	Ads	100	—	1,000	2,200	10^{-4}	10^{-4}
5	Ads	0.1	—	1,000	2,200	10^{-4}	0.1
6	Ads	0.1	—	1,000	2.2	10^{-4}	0.1
7	Ads	0.1	—	1,000	2,200	10^{-4}	10^{-4}
8	Ads	0.1	—	1,000	2.2	10^{-4}	10^{-4}
9	Con	—	100	—	—	—	—
10	Con	—	0.01	—	—	—	—

*Ads, adsorbate; Con, contaminant

Table 6. Total Product Lost During Wash Stage* for Systems in Table 5

System	Contam. Conc. at End Each Wash % Equilib. Value	Product Lost Amt. mg × 10^{-2}	Product Lost %**
1	85	6.88	4.4
2	90	6.10	3.9
3	95	4.39	2.8
4	99	3.49	2.2

*With $Sh_{p1} = 100$, $K_{D1} = 10^{-4}$ mg/cm^3
**Relative to 1.56 mg product, the total amount in particles at end of adsorption stage

Acknowledgment

The authors gratefully acknowledge partial support of this work by the National Science Foundation, Grant No. CBT-8416165.

Notation

A = adsorbate
A_i = adsorbate i, $i = 1, 2, \ldots, m$
A_o = external surface area of spherical particle = $4\pi R_o^2$, m^2
A_iL = adsorbate-ligand complex for monovalent adsorbate, $i = 1, 2, \ldots, m$

AL_j = adsorbate-ligand complex for multivalent adsorbate, $j = 1, 2, \ldots, z$
C_{di} = concentration of solute i in bulk fluid phase, kg/m^3
C_{doi} = initial concentration of solute i in bulk fluid phase, kg/m^3
C'_{di} = dimensionless concentration of solute i in bulk fluid phase = C_{di}/C_{doi}
C_L = concentration of vacant available ligands on internal surface of adsorbent, kg/m^3 particle
C'_L = dimensionless concentration of vacant available ligands on internal surface of adsorbent = C_L/C_T
$C_{L_{adj}}$ = concentration of vacant available ligands adjacent to an occupied ligand, kg/m^3 particle
$C'_{L_{adj}}$ = dimensionless concentration of vacant available ligands adjacent to an occupied ligand = $C_{L_{adj}}/C_T$
C_{pi} = concentration of solute i in pore fluid phase, kg/m^3
C'_{pi} = dimensionless concentration of solute i in pore fluid phase = C_{pi}/C_{doi}
C_{si} = concentration of solute i in adsorbed phase, kg/m^3 particle
C^*_{soi} = concentration of solute i in adsorbed phase in equilibrium with C_{doi}, kg/m^3 particle
C'_{si} = dimensionless concentration of solute $i (i = 1, \ldots, m)$ in adsorbed phase = C_{si}/C_T; dimensionless concentration of solute $i (i = m + 1, \ldots, \ell)$ in adsorbed phase = C_{si}/C^*_{soi}
$C_{s1,j}$ = concentration of multivalent solute in adsorbed phase interacting with j sites, kg/m^3 particle
$C'_{s1,j}$ = dimensionless concentration of multivalent solute in adsorbed phase interacting with j sites = $C_{s1,j}/C_T$
C_T = total concentration of available ligand, kg/m^3 particle
D_{pi} = effective pore diffusivity of solute i in pore fluid phase, m^2/s
$D_{pRi} = D_{pi}/D_{p1}$
f_i = equilibrium functions for solutes adsorbed onto ligands
$k_{1,i}$ = forward interaction rate constant of monovalent solute i, m^3/kg · s
$k_{1,1}, k_{3,1}, \ldots k_{2z-1,1}$ = forward interaction rate constants of multivalent solute, m^3/kg · s
$k'_{2j-1,1} = k_{2j-1,1}S, j = 2, 3, \ldots, z$, s^{-1}
$k_{2,i}$ = reverse interaction rate constant of monovalent solute i, s^{-1}
$k_{2,1}, k_{4,1}, \ldots k_{2z,1}$ = reverse interaction rate constants of multivalent solute, s^{-1}
K_{Ai} = association equilibrium constant of solute i, m^3/kg
K_{Di} = dissociation equilibrium constant of solute i, kg/m^3
$K_{D1,j}$ = dissociation equilibrium constant of multivalent solute interacting with j sites, kg/m^3
K_{fi} = film mass transfer coefficient of solute i, m/s
ℓ = number of solutes involved in biospecific and nonspecific adsorption
L = vacant ligand
L_{adj} = adjacent vacant ligand
m = number of solutes involved in biospecific adsorption
n = total number of solutes in finite bath
N = number of internal collocation points
$p_i(\rho)$ = concentration profile of solute i in pore fluid at end of adsorption stage
Po_i = Porath parameter for monovalent solute i, = $k_{1,i}A_o/\epsilon_p D_{pi}$, m^3/kg
$Po_{1,j}$ = Porath parameter for multivalent solute interacting with j sites, Eq. 19; m^3/kg when $j = 1$, dimensionless when $j = 2, 3 \ldots, z$
$q_i(\rho)$ = concentration profile of monovalent adsorbed species i at end of adsorption stage
r = radial distance in particle, m
R_o = radius of particle, m
Sh_{pi} = Sherwood number = $2R_o K_{fi}/\epsilon_p D_{pi}$
S = number of available ligands adjacent to each other
t = time in adsorption stage, s
t_w = time in wash stage, s
$u_j(\rho)$ = concentration profile of multivalent adsorbate interacting with j sites at end of adsorption stage
V = volume of finite bath, m^3 (volume of fluid plus volume of adsorbent particles)
z = number of active sites on multivalent adsorbate

Greek letters

δ = 0 for nonadsorbed species; 1 for species involved in nonspecific adsorption
ϵ = void fraction in finite bath
ϵ_p = void fraction in particles
ρ = dimensionless radial distance in particle, $(r/R_o)^2$
τ = dimensionless time in adsorption stage = tD_{p1}/A_o
τ_w = dimensionless time in wash stage = $t_w D_{p1}/A_o$

Subscripts

d = bulk fluid
i = integer
j = integer
p = pore fluid
s = solid
w = wash stage
o = initial value

Literature cited

Arnold, F. H., H. W. Blanch, and C. R. Wilke, "Analysis of Affinity Separations. I: Predicting the Performance of Affinity Adsorbers," *Chem. Eng. J.*, **30**(2), B9 (1985a).

———, "Analysis of Affinity Separations. II: The Characterization of Affinity Columns by Pulse Techniques," *Chem. Eng. J.*, **30**(2), B25 (1985b).

Arve, B. H., "The Modelling and Analysis of Multicomponent, Multivalent Biospecific Adsorption," Ph.D. Diss., Univ. Missouri, Rolla (1986).

Balzli, M. W., A. I. Liapis, and D. W. T. Rippin, "Application of Mathematical Modelling to the Simulation of Multicomponent Adsorption in Activated Carbon Columns," *Trans. Inst. Chem. Eng.*, **56**, 145 (1978).

Blakebrough, N., *Biochemical and Biological Engineering Science*, Academic Press, New York, **1** (1967).

Calderbank, P. H., and S. J. R. Jones, "Physical Rate Processes in Industrial Fermentation. III: Mass Transfer from Fluids to Solid Particles Suspended in Mixing Vessels," *Trans. Inst. Chem. Eng.*, **39**, 363 (1961).

Calderbank, P. H., and M. B. Moo-Young, "The Continuous Phase Heat and Mass-Transfer Properties of Dispersions," *Chem. Eng. Sci.*, **16**, 39 (1961).

Carslaw, H. C., and J. C. Jaeger, *Conduction of Heat in Solids*. Clarendon, Oxford (1959).

Chase, H. A., "Affinity Separations Utilizing Immobilized Monoclonal Antibodies—A New Tool for the Biochemical Engineer," *Chem. Eng. Sci.*, **39**, 1099 (1984a).

———, "Predictions of the Performance of Preparative Affinity Chromatography," *J. Chromatog.*, **297**, 179 (1984b).

Eilat, D., and I. M. Chaiken, "Expression of Multivalency in the Affinity Chromatography of Antibodies," *Biochemistry*, **18**(5), 791 (1979).

Eveleigh, J. W., and D. E. Levy, "Immunochemical Characteristics and Preparative Application of Agarose-Based Immunosorbents," *J. Solid-Phase Biochem.*, **2**(1), 45 (1977).

Frej, A.-K., J.-C. Gustafesson, and P. Hedman, "Recovery of β-Galactosidase by Adsorption from Unclarified Escherichia coli Homogenate," *Biotechnol. Bioeng.*, **28**, 133 (1986).

Froment, G. F., and L. Hosten, "Catalytic Kinetics: Modelling," *Catalysis Science and Technology*, J. R. Anderson and M. Boudart, eds., Springer-Verlag, New York, **2** (1981).

Geankoplis, C. J., *Transport Processes and Unit Operations,* 2nd ed., Allyn and Bacon, Boston (1983).
Hill, E. A., and M. D. Hirtenstein, "Affinity Chromatography: Its Application to Industrial-Scale Processes," *Adv. Biotech. Proc.,* **1,** 31 (1983).
Hougen, O. A. and K. M. Watson, *Chemical Process Principles,* Wiley, New York (1947).
Janson, J.-C., "Large-Scale Affinity Purifications—State of the Art and Future Prospects," *Trends in Biotechnol.,* **2**(2), 1 (1984).
Janson, J.-C., and P. Hedman, "Large-Scale Chromatography of Proteins," *Adv. Biochem. Eng.,* **25,** 43 (1982).
Janson, J.-C., and L.-E. Nystrom, "Biokemiska Separationsmetoder i Stor Skala," *Kemisk Tidskrift,* no. 12, 41 (1985) (in Swedish).
Katoh, S., T. Kambayashi, R. Deguchi, and F. Yoshida, "Performance of Affinity Chromatography Columns," *Biotechnol. Bioeng.,* **20,** 267 (1978).
Klaus, R. A., "A Computer-Based Methodology for Regression and Experimental Design with Nonlinear Algebraic and Ordinary Differential Equation Multiresponse Models," Ph.D. Diss., E. T. H. Zurich (1981).
Liapis, A. I., and R. J. Litchfield, "A Note on the Off-Diagonal Terms of the Effective Pore Diffusivity Matrix," *Trans. Inst. Chem. Eng.,* **59,** 122 (1981).
Liapis, A. I., and D. W. T. Rippin, "The Simulation of Binary Adsorption in Activated Carbon Columns Using Estimates of Diffusional Resistance within the Carbon Particles Derived from Batch Experiments," *Chem. Eng. Sci.,* **33,** 593 (1978).
Michelsen, M. L., "An Efficient General-Purpose Method for the Integration of Stiff Ordinary Differential Equations," *AIChE J.,* **22,** 594 (1976).
Nygren, H., and M. Stenberg, "Kinetics of Antibody-Binding to Surface-Immobilized Antigen: Influence of Mass Transport on the Enzyme-Linked Immunosorbent Assay (ELISA)," *J. Colloid Interface Sci.,* **107**(2), 560 (1985).
Parikh, I., and P. Cuatrecasas, "Affinity Chromatography," *Chem. Eng. News,* 17 (Aug. 26, 1985).
Porath, J., and T. Kristiansen, "Biospecific Affinity Chromatography and Related Methods," *The Proteins,* H. Neurath, and R. L. Hill, eds., Academic Press, New York, **1** (1975).
Seinfeld, J. H., and L. Lapidus. *Mathematical Methods in Chemical Engineering,* Prentice Hall, Englewood Cliffs, NJ (1974).
Sorber, H. A., *Handbook of Biochemistry, Selected Data for Molecular Biology,* Chemical Rubber Co., Cleveland (1968).
Sportsman, J. R., J. D. Liddil, and G. S. Wilson, "Kinetic and Equilibrium Studies of Insulin Immunoaffinity Chromatography," *Anal. Chem.,* **55,** 771 (1983).
Tsou, H-S., and E. E. Graham, "Prediction of Adsorption and Desorption of Protein on Dextram Based Ion-Exchange Resin," *AIChE J.,* **31,** 1959 (1985).
Villadsen, J., and M. L. Michelsen, *Solution of Differential Equation Models by Polynomial Approximation,* Prentice Hall, Englewood Cliffs, NJ (1978).

Manuscript received Apr. 3 and May 20, 1986 and revision received Aug. 15, 1986.